
Title: Influence of Zr content on phase transformation, microstructure and mechanical properties of $Ti_{75-x}Nb_{25}Zr_x$ ($X = 0\sim6$) alloys

Authors: Zhou Yu, Li Yuxuan, Yang Xianjin, Cui Zhenduo, Zhu Shengli

PII: S0925-8388(09)01369-3
DOI: doi:10.1016/j.jallcom.2009.07.006
Reference: JALCOM 20276

To appear in: *Journal of Alloys and Compounds*

Received date: 28-5-2009
Revised date: 1-7-2009
Accepted date: 2-7-2009

# Influence of Zr content on phase transformation, microstructure and mechanical properties of Ti-25Nb-xZr(X=0~6) alloys

ZHOU Yu, YANG Xianjin*, CUI Zhenduo, ZHU Shengli
School of Materials Science and Engineering, Tianjin University,
Tianjin 300072, P. R. China

## Abstract

Ternary Ti-Nb-Zr alloys consisting of biocompatible alloying elements have been prepared to investigate the effect of Zr content on β→α phase transformation, microstructure and mechanical properties. The study showed that element Zr could stablize β phase and its effect on β phase transus exhibited a "margin effect". With the increasing of Zr content, microstructure of Ti-Nb-Zr alloy was refined and the strength of ternary Ti-Nb-Zr alloys also improved while the plasity of Ti-Nb-Zr alloys significantly decreased. Ti-25Nb-3Zr alloy exhibited the maximum ultimate tensile strengh about 775Mpa and Ti-25Nb-2Zr exhibited the lowest elactic modulus about 62 GPa. The possible reasons for lower elastic modulus of Ti-25Nb-(2~3)Zr alloys were also discussed.



**Keywords:** A: metals; C: X-ray diffraction; D: dental alloys

## Introduction

Ti-6Al-4V and Ni-Ti alloys have been widely used as permanent implant materials in

* Correspondence Author: YANG Xianjin, email: xjyang@tju.edu.cn, Tel: +86-22-27405602, Fax: +86-22-27891371

the replacement of hard tissues, such as in artificial joints and dental implants, due to their excellent corrosion resistance, high strength and reasonable elastic modulus among the metal-based biomaterials. Even though these alloys have been registered in ASTM standards for biomedical application, surface modification is necessary for these alloys as Al, V, and Ni are known to be toxic elements. Especially, the wear debris of Ti-6Al-4V alloy generated by long-term application in human body has been found to promote osteolytic mediators, resulting in aseptic loosening of prostheses in the in vitro studies [1-4]. As a result, new Ti-based alloys with non-toxic elements such as Nb, Zr, Ta, Sn etc have been developed in order to solve the above problems and possess shape memory and superelasic effects etc[5-12]. Recently, Many β type Ti-base alloys exhibiting better mechanical properties have been studied and found to exhibit both better tensile properties and lower elastic modulus than other metal based biomaterials, e.g., Ti–Ta base alloys [13-15], Ti–Mo base alloys [16, 17 ] and Ti–Nb base alloys[18-20]. It is confirmed that mechanical properties can be improved by addition of further alloying elements to these binary alloys.

It was reported that Ti-25Nb alloy exhibited shape memory effect and superelastic behavior at room temperature and its martensite transformation start temperature was around room temperature [22] which means it is a promising candidate for replacing Ni-Ti alloy for biomedical application with further alloy optimization. In the present study, element Zr was chosen as a ternary alloying element to Ti-25Nb (at%) alloy for its excellent biocompatibility and similar atomic lattice parameters with element Ti which could reduce the solution hardening effects compared with other alloying elements. Therefore, desirable mechanical properties could be obtained by optimizing alloy composition and thermo-mechanical processing methods.

## Experimental procedure

Ti-25Nb-(0-6)Zr alloys were prepared with pure( 99.9%)Ti, Nb and Zr. Small alloy ingots of 30mm in diameter were melted by vacuum arc melting on a water-cooled copper hearth under an argon gas atmosphere with a non-consumable tungsten electrode. The ingots were re-melted at least five times to ensure the chemical homogeneity. Then, these ingots were hot forged at 1273K to bars with section dimension of 13mm×13mm. After that, these bars were solution treated in salt bath consisting of NaCl and KCl mixtures at 1123K for 1h, followed by rapid quenching into water. The oxidation layer on the surface of alloy bars was removed by mechanically grounding. Samples for chemical composition analysis, microstructural observation, and tensile tests were prepared by electro-discharge machine. The specimens for optical observations were prepared following standard metallographic techniques used for titanium and its alloys and etched with Kroll's reagent (5 ml HF, 10 ml $HNO_3$ and 85 ml $H_2O$). Differential scanning calorimetry (DSC) was performed at a constant heating rate of 5 K/min in an Ar atmosphere to measure the phase transformation behavior by NETZSCH DSC 404C.The phase structure of alloys as studied were detected using a RIGAK/DMAX2500 X-ray diffractometer with CuK-radiation and XRD patterns were collected in the 2θ ranges from 30 to 90◦. Tensile tests were conducted at a strain rate of $1.5\times10^{-4}$ $s^{-1}$ at room temperature, and the gage length and width were 25mm and 3mm, respectively.

## Results and discussion

Fig.1. DSC heating curves of Ti-25Nb-(0-6)Zr alloys quenched from 1123K

Fig.1 shows the DSC heating curves at a constant heating rate of 5K/min in quenched Ti-25Nb-(0-6)Zr alloys. Ti-25Nb exhibits an endothermic peak near 753K which gradually decreased after 660K, and an exothermic peak near 793K followed by the endothermic peak; Ti-25Nb-2Zr exhibited an endothermic peak near 723K which gradually decreased after 665K, and an exothermic peak near 768K followed by the endothermic peak Ti-25Nb-4Zr exhibited an endothermic peak near 705K which has gradually decreased after 660K; Ti-25Nb-6Zr exhibits an endothermic peak near 691K and an exothermic peak near 733K followed by the endothermic peak; The shift of endothermic peak with increasing Zr content indicated the change of β phase transus. Although Zr is generally considered as neutral element, it exhibited effects of stabling β phase and depressing β phase transus in this study. Moreover, the effect of Zr on β phase transus exhibit a "margin effect", which means the results show that β stabling effects of element Zr on this alloy will weaken noticeably with the addition of more Zr element. As shown in Fig.1, while β phase transus continued to be lowered as more and more Zr was added, its effect of stabling β phase was diminishing: from 0~2at%, 2~4at%, 4~6at% Zr, β phase transus was lowered by 30K, 18K, 14K respectively. However, these results may not apply to all titanium alloys as literature indicates that the effect of

Zr on titanium alloys may vary significantly with different main alloy elements (mainly refers to β or α stabling elements).

Fig.2. Optical micrographs of Ti-25Nb-xZr as-cast alloys:

x=(a) 1 (b) 2 (c) 3 (d) 4 (e) 6

The microstructures shown in Fig.2 are taken from the same position of the ingots of Ti-25Nb-xZr as-cast alloys. According to Fig. 2, no trace of martensite and α phase were observed in the microstructure of these solution treated specimen. These alloys are mainly composed of typical equiaxial β phase. With the increasing of Zr content, the microstructures of alloys tend to be refined.

Fig.3 XRD Patterns of Solution treated Ti-25Nb-(0-6)Zr Alloys

Fig.3 shows the XRD patterns of Ti-25Nb-(0-6)Zr alloy samples in which solution treatment was carried out at 1123K for 1 hour followed by room temperature water quenching(WQ). The patterns indicated that the crystal composition of these alloys barely changed which means that crystal structures of Ti-25Nb-xZr alloys are not sensitive to their Zr contents. Diffraction peaks corresponding to the α phase cannot be observed in all alloys. In Ti-25Nb-(3-6)Zr alloys, only the peaks of the β phase were observed. This means that the $M_s$ of these alloys are below room temperature. However, the peaks of α'' phase were observed in Ti-25Nb and Ti-25Nb-Zr alloys, indicating that the $M_s$ of these alloys are above room temperature. This means that the martensitic transformation temperature has been decreased as Zr content increases. Because of a small enthalpy of the martensitic transformation and a large difference between $M_s$ and $M_f$, it was difficult to obtain a transformation peak by a differential calorimeter in the solution-treated alloys. Kim etc reported [22] that in Ti-22Nb-(2-8)Zr alloys, the martensitic transformation start temperature decreased by 38K with 1at% increase of Zr content. Meanwhile, this also indicates the effects of Zr to stabilize β phase: with increasing Zr content in Ti-25Nb-xZr alloys, α'' phase decreased and when Zr content was above 2%, the α'' phase was completely eliminated and the β phase was fully retained.

Fig.4 Lattice Parameters of β phase of solution treated Ti-25Nb-(0-6)Zr alloys

The lattice parameters of bcc-structured β phase are plotted in Fig. 4 as a function of Zr content in Ti-25Nb-xZr (x=0~6). The lattice parameter increases monotonously with increasing Zr content. As the atomic sizes of Ti, Nb, and Zr are 0.145 nm, 0.147 nm and 0.160 nm, respectively, it suggests that Zr atom is soluble in the bcc-structured β phase, and up to 6 at.% of Zr content is within the solubility limit in the Ti-25Nb alloy.

Fig.5 Strain-Stress Curves of Ti-25Nb-(0~6)Zr alloys obtained at R.T

Fig.5 shows stress-strain curves of Ti-25Nb-(0~6)Zr alloys obtained by tensile tests at room temperature after the solution treatment at 1123K for 1 hour followed by water quenching. In Fig.5, all alloys exhibited single-stage yielding. Premature failure was observed in the specimens of Ti-25Nb-(3~6)Zr alloys. The elongation monotonously decreased from 23% to 4% with increasing Zr content, while the strength first increased with increasing Zr content till it reached 3% and then it began to decrease. This is due to the solid-solution hardening by the addition of Zr. The largest elongation of 23% was obtained in the Ti-25Nb alloy and the highest ultimate strength of 775MPawas attained in the Ti-25Nb-3Zr alloy. According to the test results, Ti-25Nb-(1~2)Zr alloy has the best combination of plasticity and strength.

Fig.6 shows the effect of Zr content on ultimate strength and elastic modulus of Ti-25Nb alloy. The Zr content dependence on elastic modulus is the reverse of that on ultimate strength. The lowest elastic modulus of 62 GPa was obtained in the Ti-25Nb-2Zr alloy. The elastic modulus of metastable β titanium alloy is mainly influenced by its phase constitution. So the elastic modulus of titanium alloy will increase with the volume fraction of high modulus component. Among all the phases in titanium alloys, the relative comparison of elastic modulus is ω>α’>α>β>α”[21]. According to the effect of Nb and Zr content to the martensite transformation temperature of titanium alloys reported by Kim etc [22, 23], the $M_s$ of Ti-25Nb-(2-3)Zr alloy is around room temperature. Hence, during tensile tests, stress induced martensite transformation may occur in Ti-25Nb-(2~3)Zr alloy and lead to the deposition of α" phase (shown in Fig.7) which will substantially lower the elastic modulus of the alloy.

Generally, in titanium alloys, as elastic modulus of β phase is much lower than that of α phase, low elastic modulus is usually obtained by adding β stabilizing elements into alloys to reduce the amount of α phase. However, Element Zr, an element widely considered as neutral, is recognized to be effective in lowering elastic modulus of titanium alloy. This may be explained as follows: first, as results of this study showed that the β phase transus temperature is averagely decreased by 10K with 1at% increase of Zr content. This means that Zr also stabilizes beta titanium alloy although its effects is not so apparent as typical β stabilizers which indicate it could reduce elastic modulus of titanium alloy; second, as indicated in this work, Zr could decrease martensitic transformation start temperature. When $M_s$ is lowered to room temperature, it is easier for the deposition of stressed induced martensite (a''). So when deformed, these alloys tend to exhibit lower elastic modulus. Also, the ω phase suppressing effect of Zr element in titanium alloys may contribute to lower elastic modulus of titanium alloys in this study. Although no evidence indicate that the ω phase exists in Ti-25Nb-xZr alloys in this study, its existence should not be ruled out because of its nature of small amount and its form of fine particles.

Fig.6 Effect of Zr content on the ultimate strength and elastic modulus of Ti-25Nb alloy

Fig.7 XRD Patterns of tensile test specimen of Ti-25Nb-(0~6)Zr Alloys

Fig.8 Fracture surface morphologies of Ti-25Nb-2Zr (a), (b) and Ti-25Nb-6Zr (c), (d) alloys tensile test specimen after solution treatment

Fig.8 shows fracture surface morphologies of solution-treated Ti-25Nb-2Zr (a), (b) and Ti-25Nb-6Zr (c), (d) alloys subjected to tensile tests. The fracture morphologies of Ti-25Nb-2Zr alloy mainly exhibited tough fracture characteristics and Ti-25Nb-6Zr exhibited brittle fracture characteristics. Ti-25Nb-2Zr tolerated about 13% elongation before failure occurred. As shown in Fig. 7(a) and (b), mainly equiaxial and deep dimples appeared on the fracture morphology, while Fig. 7 (c) and (d) showed transcrystalline fracture and small and shallow dimples. The characteristic of fracture surfaces correspond well with those of tensile properties.



## Conclusions

In Ti-Nb-Zr tenary alloys, the effect of Zr content on the microstructure and mechanical properties has been investigated by optical microscopy, differential scanning calorimetry, X-ray diffraction and tensile test. The following conclusions have been obtained:

(1) Element Zr can stablize β phase and this effect exhibit a “margin effect”: as more Zr was added (2at%, 4at% and, 6at%), its β stabling effect was diminishing (β phase transus was lowered by 30K, 18K, 14K respectively).

(2) The microstructure of ternary Ti-Nb-Zr alloys tended to be refined after the addition of Zr element.

(3) Zr suppresses the desposition of α’’ phase in quenched ternary Ti-Nb-Zr alloys. As Zr content increases above 2%, α’’ phase is completely eliminated and the β phase is fully stabilized.

(4) With increasing Zr content, the lattice parameter increases monotonously and the strength of ternary Ti-Nb-Zr alloys is improved while the plasity of Ti-Nb-Zr alloys significantly decreases. This is attributed to the solid-solution hardening by the addition of Zr. Ti-25Nb-3Zr alloy exhibits the maximum ultimate tensile strengh about 775Mpa and Ti-25Nb-2Zr exhibits the lowest elactic modulus about 62 GPa.

(5) Stress induced martensite transformation occured in Ti-25Nb-(2~3)Zr alloys during tensile tests and leads to the deposition of α’’ phase during tensile test which may contribute to the low elastic modulus of these alloys.

## Reference

[1] Black J. J Bone Jt Surg 1988;70B:517.

[2] Wapner KL. Clin Orthop 1991;271:12.

[3] Eisenbarth E, Breme J, Hildebrand H. Biomaterialien 2001;2(4).

[4] Rogers D, Howie DW, Graves SE, Pearcy MJ, Haynes DR. J Bone Jt Surg 1997;79B:311.

[5] T. Grosdidier, M.J. Philippe, Mater. Sci. Eng. A291 (2000) 218–223.

[6] E. Takahashi, T. Sakurai, S. Watanabe, N. Masahashi, S. Hanada, Mater. Trans. 43 (2002) 2978–2983.

[7] T. Maeshima, M. Nishida, Mater. Trans. 45 (2004) 1096–1100.

[8] T. Zhou, M. Aindow, S.P. Alpay, M.J. Blackburn, M.H. Wu, Scripta Mater. 50 (2004) 343–348.

[9] H.Y. Kim, Y. Ohmatsu, J.I. Kim, H. Hosoda, S. Miyazaki, Mater. Trans. 45 (2004) 1090–1095.

[10] H. Hosoda, Y. Fukui, T. Inamura, K. Wakashima, S. Miyazaki, K. Inoue, Mater. Sci. Forum 426–432 (2003) 3121.

[11] Y. Fukui, T. Inamura, H. Hosoda, K. Wakashima, S. Miyazaki, Mater. Trans. 45 (2004) 1077–1082.

[12] T. Inamura, Y. Fukui, H. Hosoda, K. Wakashima, S. Miyazaki, Mater.Trans. 45 (2004) 1083–1089.

[13] Y. L. Zhou, N. Mitsuo, A. Toshikazu, Mater. Sci.Eng. A371(2004) 283~290

[14] Y. L. Zhou, N. Mitsuo, A. Toshikazu, Mater. Sci.Eng. A384(2004) 92~101

[15] M. Ikeda,S. Komatsu,Y. Nakamura, Mater. Trans. 45(2004) 1106~1112

[16] L.D. Zardiackas, D.W. Mitchell, J.A. Disegi, ASTM Symp.on Medicial Applications of Titanium and Its Alloys,The Material and Biological Issues, 1994,11:15~16

[17] J. Lin, J.H. Chern Lin, C.P. Ju, Biomaterials23 (2002) 723~1730

[18] H. Hosoda, Y. Fukui, T. Inamura, K. Wakashima, S. Miyazaki, K.Inoue, Mater. Sci. Forum 425–432 (2003) 3121–3125.

[19] J.I. Kim, H.Y. Kim, Y. Ohmatsu, H. Hosoda, S. Miyazaki, Collected Abstracts of the 2003 Fall Meeting of Japan Institute of Metals, pp.149.

[20] J.I. Kim, H.Y. Kim, H. Hosoda, S. Miyazaki, Mater. Trans. 46 (2005) 852–857

[22] J.I. Kim, H.Y. Kim, T. Inamura, H. Hosoda, S. Miyazaki, Mater. Sci.Eng. A403 (2005) 334–339

[21] W.F. Ho, C.P. Ju, J.H. Chern Lin, Biomaterials 20(1999) 2115-2122

[23] H. Y. Kim, Y. Ikehara, J.I. Kim, H. Hosoda , S. Miyazaki, Acta Mater. 54(2006) 2419–2429

## Figure Captions

Figures list

Fig.1. DSC heating curves of Ti-25Nb-(0-6)Zr alloys quenched from 1123K

Fig.2. Optical micrographs of Ti-25Nb-xZr as-cast alloys: x=(a) 1 (b) 2 (c) 3 (d) 4 (e) 6

Fig.3 XRD Patterns of Solution treated Ti-25Nb-(0-6)Zr Alloys

Fig.4 Lattice Parameters of β phase of solution treated Ti-25Nb-(0-6)Zr alloys

Fig.5 Strain-Stress Curves of Ti-25Nb-(0~6)Zr alloys obtained at R.T

Fig.6 Effect of Zr content on the ultimate strength and elastic modulus of Ti-25Nb alloy

Fig.7 XRD Patterns of tensile test specimen of Ti-25Nb-(0~6)Zr Alloys

Fig.8 Fracture surface morphologies of Ti-25Nb-2Zr (a), (b) and Ti-25Nb-6Zr (c), (d) alloys tensile test specimen after solution treatment

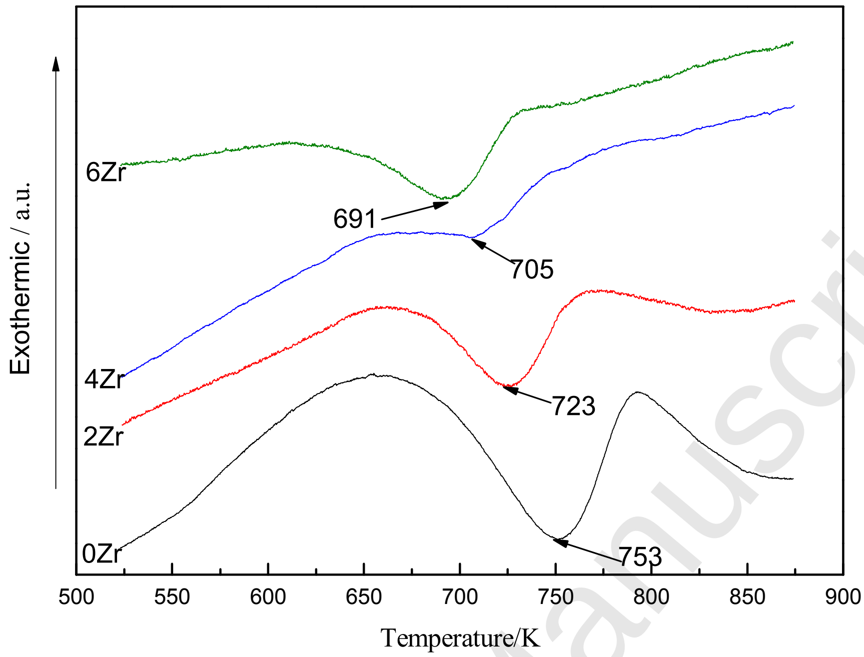


Fig.1. DSC heating curves of Ti-25Nb-(0-6)Zr alloys quenched from 1123K

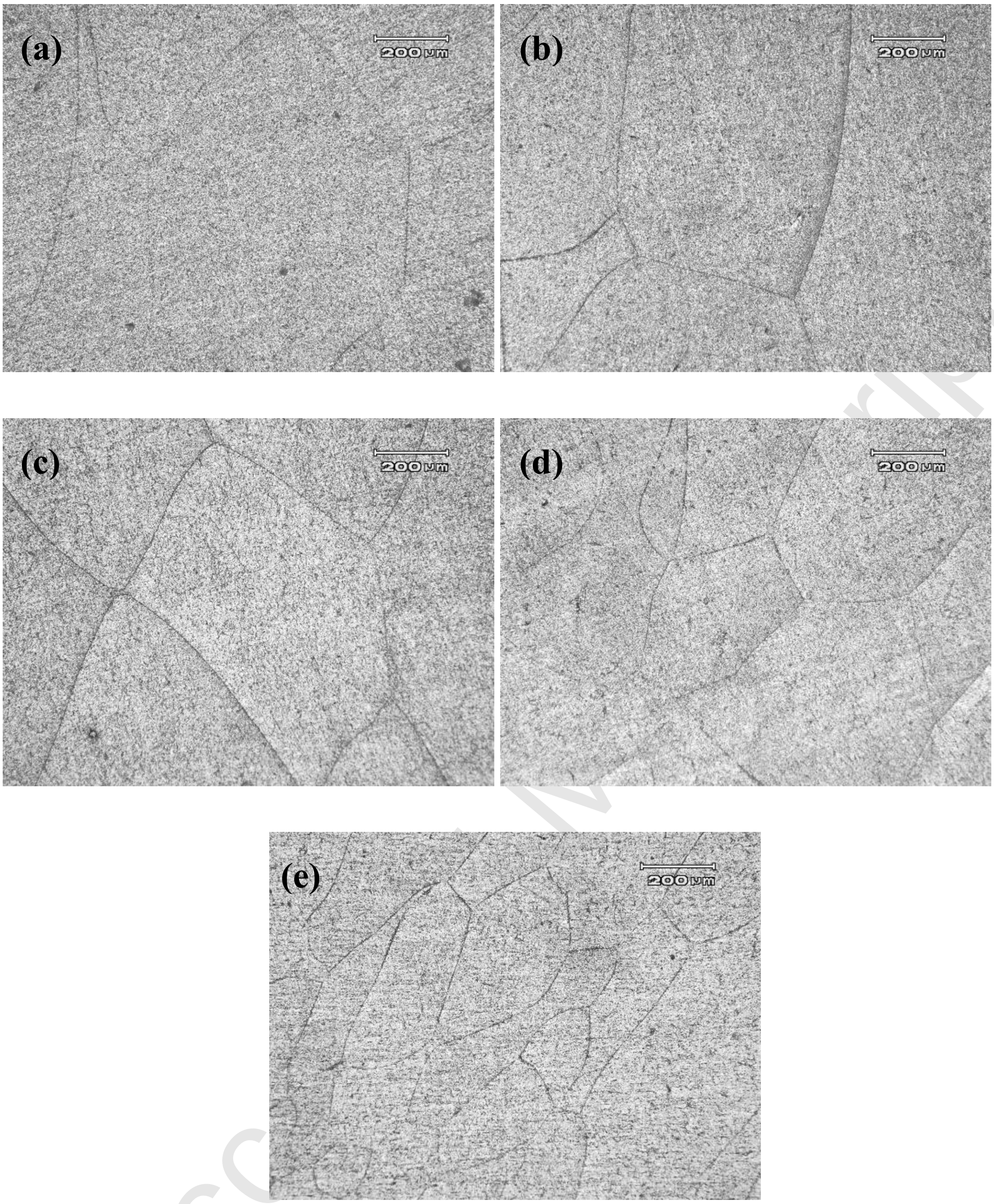


Fig.2. Optical micrographs of Ti-25Nb-xZr as-cast alloys:
x=(a) 1 (b) 2 (c) 3 (d) 4 (e) 6

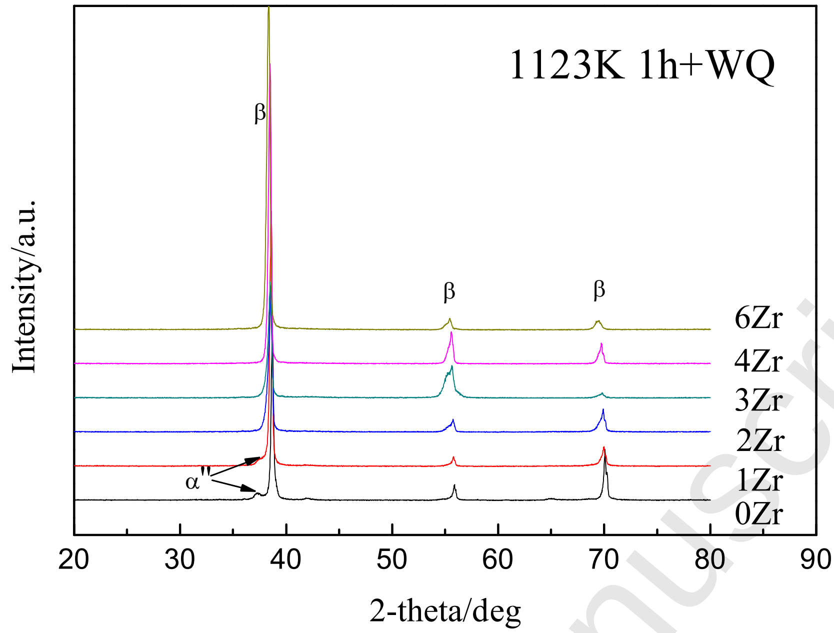


Fig.3 XRD Patterns of Solution treated Ti-25Nb-(0-6)Zr Alloys

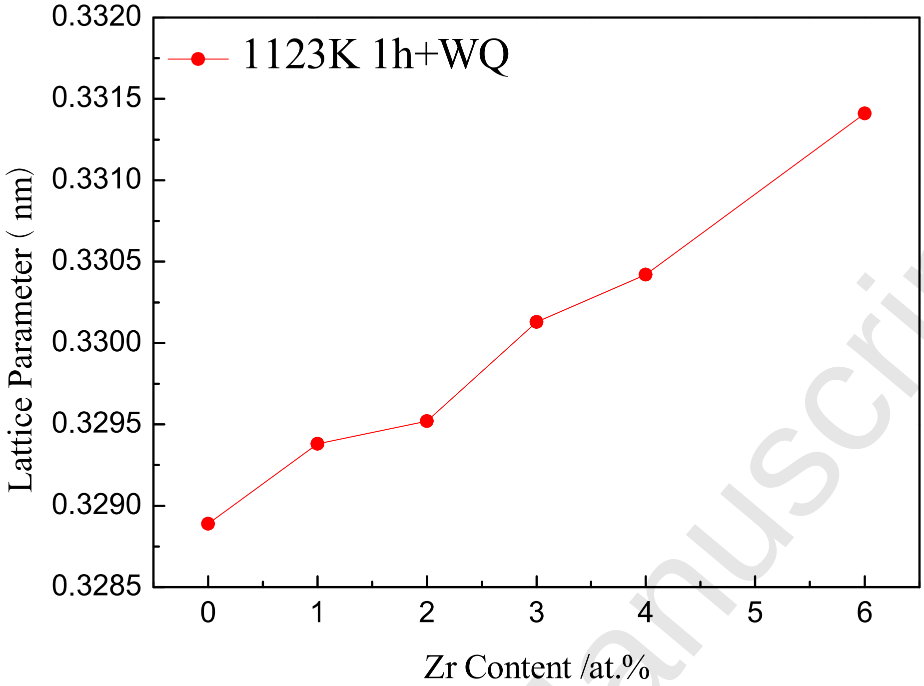


Fig.4 Lattice Parameters of β phase of solution treated Ti-25Nb-(0-6)Zr alloys

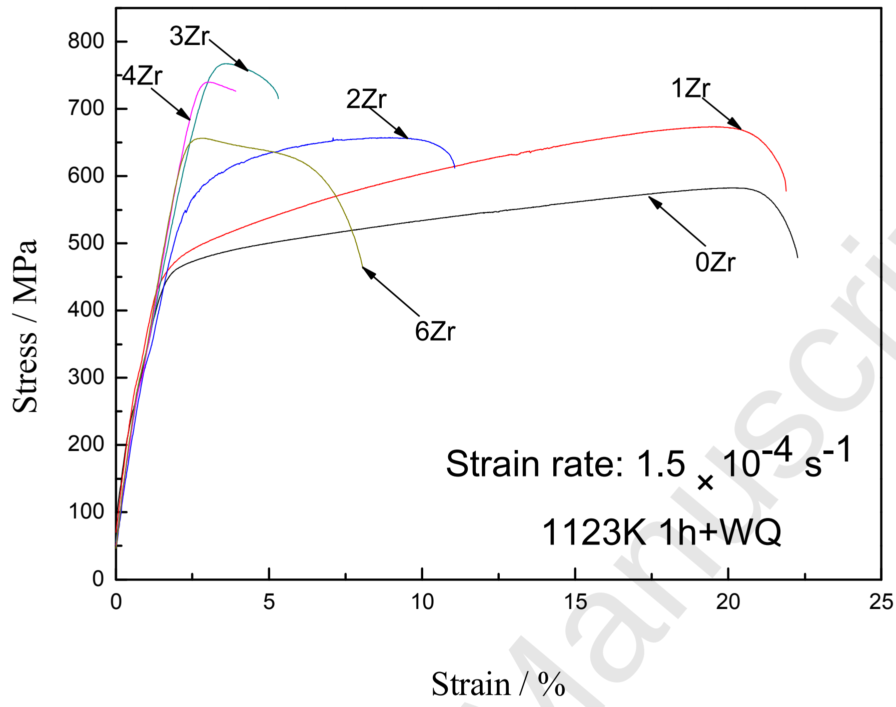


Fig.5 Strain-Stress Curves of Ti-25Nb-(0~6)Zr alloys obtained at R.T

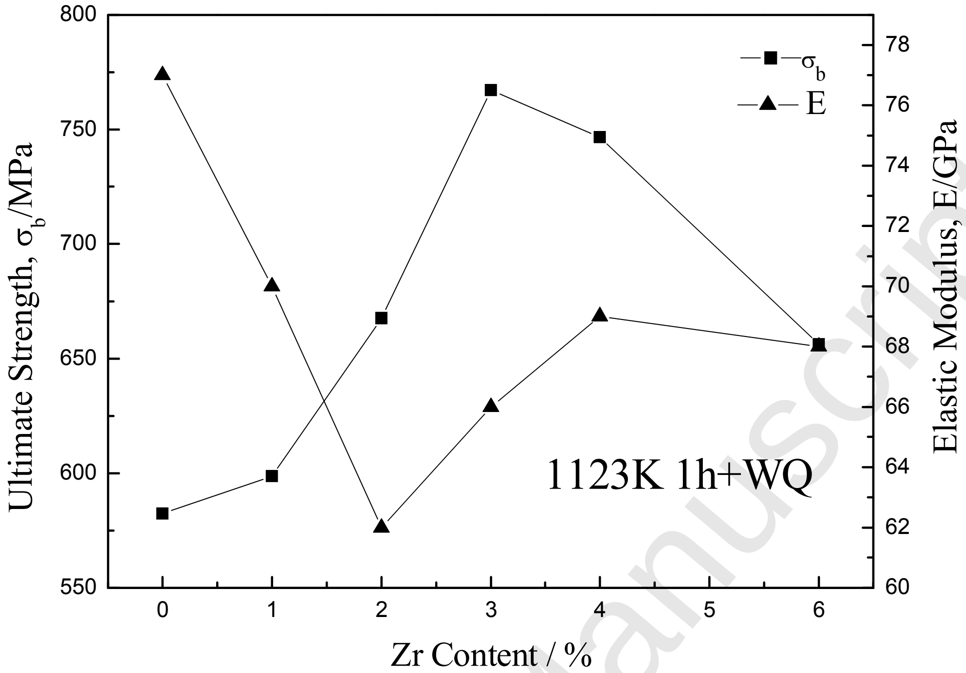


Fig.6 Effect of Zr content on the ultimate strength and elastic modulus of Ti-25Nb alloy

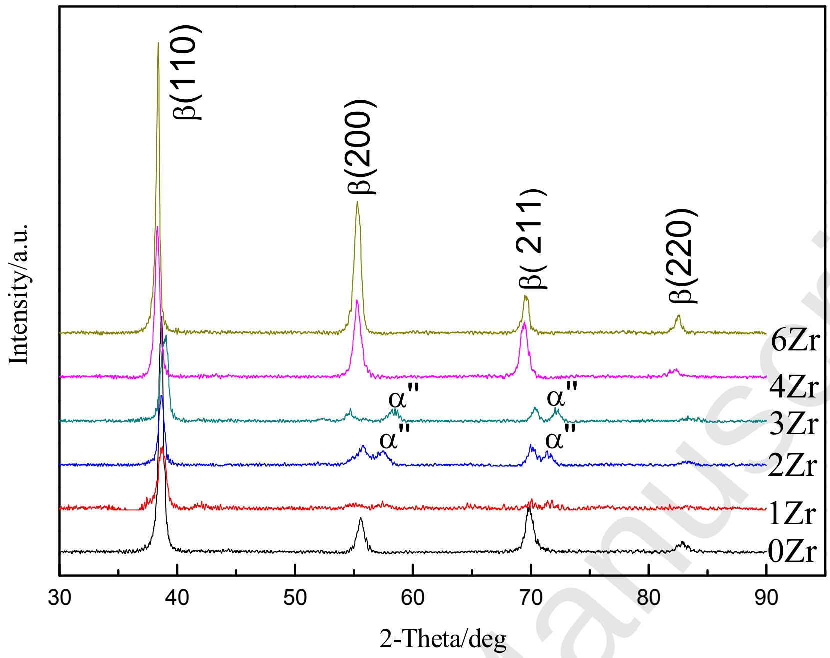


Fig.7 XRD Patterns of tensile test specimens of Ti-25Nb-(0~6)Zr Alloys

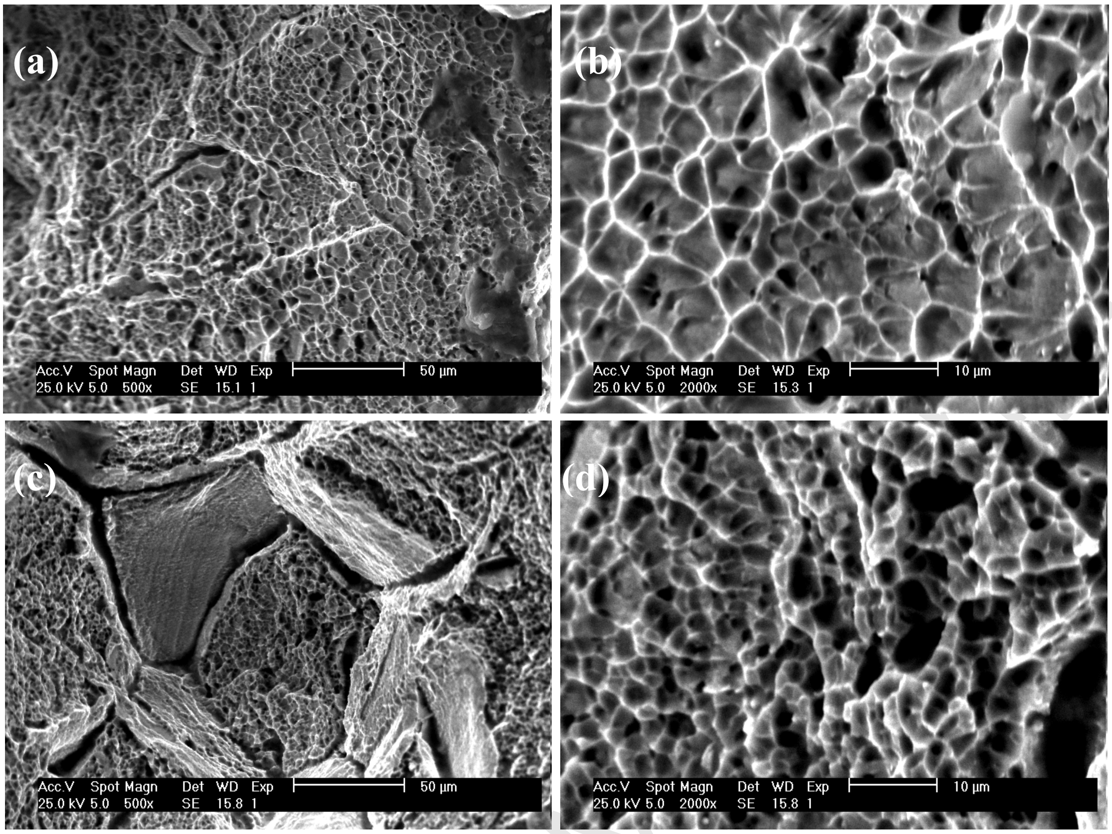


Fig.8 Fracture surface morphologies of Ti-25Nb-2Zr (a), (b) and Ti-25Nb-6Zr (c), (d) alloys tensile test specimen after solution treatment